Islamic Azad University

Journal of

Optoelectronical Nanostructures

Summer 2023 / Vol. 8, No. 3

Research Paper

Design and simulation of metal-insulator-metal waveguide for filtering and sensor applications

Asieh Karimi[1], Masoud Jabbari*[,1], Gahraman Solookinejad[2]

[1] Department of Electrical Engineering, Marvdasht branch, Islamic Azad Universty, Marvdasht, Iran

[2] Department of physics, Marvdasht branch, Islamic Azad Universty, Marvdasht, Iran

Received: 14 Jul. 2023
Revised: 17 Aug. 2023
Accepted: 4 Sep. 2023
Published:15 Sep. 2023

Use your device to scan and read the article online

Keywords:
Plasmonic,MIM, Waveguide, Filter.

Abstract

Plasmons in nanometer structures are caused by the interaction between electromagnetic waves and electrons on the metal surface. In this article, a comprehensive and detailed investigation of the effect of effective parameters on the performance of structured MIM waveguides (metal-insulator-metal) has been carried out. These structures are widely used in sensor applications based on refractive index changes or filters. This paper examines the impacts of altering factors like waveguide size, metal type, and insulation while also proposing novel structures with circular and square resonators,Then we simulated the structure of the MIM waveguide connected to the cavity of the T-shaped resonator for different values for the length L of the cavity, It is possible that this issue has a good use in filters and systems with high bandwidth to separate channels . Also,the properties of surface plasmon polaritons emission were investigated in the case where a resonator is vertically connected to it. The transmission diagram had compared to the MIM waveguide without resonator.

Citation: Asieh Karimi, Masoud Jabbari, Gahraman Solookinejad. Design and simulation of metal-insulator-metal waveguide for filtering and sensor applications. **Journal of Optoelectronical Nanostructures.** 2023; 8 (3): 90- 109. **DOI:** 10.30495/JOPN.2023.31705.1284

***Corresponding author:** Masoud Jabbari
Address: Department of Electrical Engineering, Marvdasht branch, Islamic Azad Universty, Marvdasht, Iran. **Tell:** **Email:** paper.jabari.2021@gmail.com

1. INTRODUCTION

Investigations on the propagation properties of surface plasmon polariton modes as a practical filter and optical sensor based on a plasmonic waveguide with a T-shaped resonator, symmetric surface plasmon polariton waveguides in aluminum gallium arsenide/ silver/ aluminum gallium arsenide waveguides [1], gold/alumina/waveguide gold [2] and symmetric metal-insulator-metal structures [3] as well as waveguide designs with surface plasmon polaritons have been studied so far [4]. In other studies, the analysis of surface plasmon polariton modes in insulator-metal-insulator planar plasmonic waveguides as well as the properties of insulator-metal-insulator plasmonic waveguides with a double network have been investigated [5, 6]. In other similar studies, the effect of the metal cylinder in the slot on the transmission characteristics of the metal-insulator-metal waveguide has been investigated [7, 8], and the effects of the size, location and shape of the metal cylinder in the slot waveguide on the transmission characteristics at a specific wavelength have been investigated [8, 9]. A surface plasmon polariton wave splitter has also been designed by using a metal-insulator waveguide [10,12].

Generally,To obtain of modulation depth and low insertion loss, between proposed devices in advanced THz communication systems, plasmonic devices is good candidate. Plasmonic device as a novel strategies for fast and tunable modulators were reported, recently [13].

In this paper, We first simulate a metal-insulator-metal (MIM) plasmonic waveguide and obtain and show the transmission spectrum of this structure for different metals, insulators, and changing the width of the waveguide by using Finite Element Method (FEM) and Comsol software. After that, to investigate the effect of resonators on the optical response of the waveguide, we simulated the structure with a vertical stub coupled to the main waveguide and tested the effects of changing the refractive index, changing the shape of the stub, and creating a distance between the stub and the main waveguide. Then, in addition to the stub coupled to the main waveguide, we also placed a resonator cavity on top of the stub and obtained the transmission spectrum in different shapes of this cavity and the change in the size of this cavity. [14, 15]

2-METAL-INSULATOR-METAL (MIM) WAVEGUIDE SIMULATION

In this article, we have designed a two-dimensional cylindrical waveguide structure with 100 nm wide whose surrounding metal is silver and the interior of

the waveguide is air as shown in Fig. 1. Figure (2) shows the transmission spectrum of this waveguide without any resonator. The transmission spectrum in the range of 400nm-1600nm wavelengths has never reached zero, and even from the wavelength of 800nm onwards, its transmission efficiency is above 90%. The reason for this complete transmission spectrum is that the emitted light and the resonant wavelength of the structure are far apart and there is no interference between them.

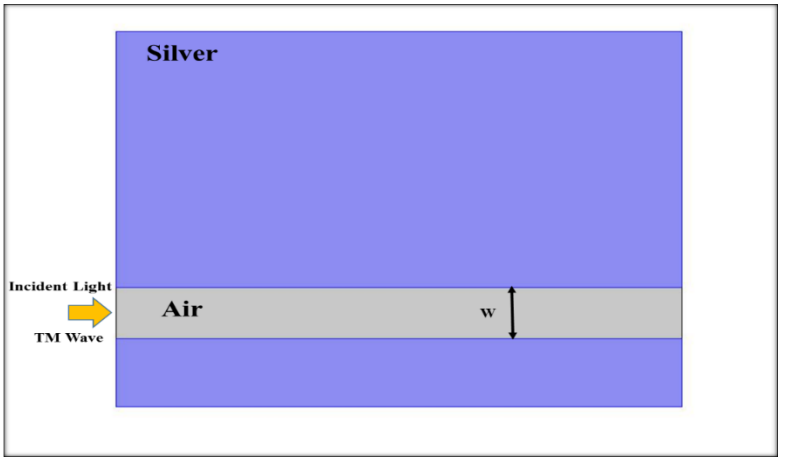

Fig 1. Waveguide structure (MIM) with a width of 100 nm.

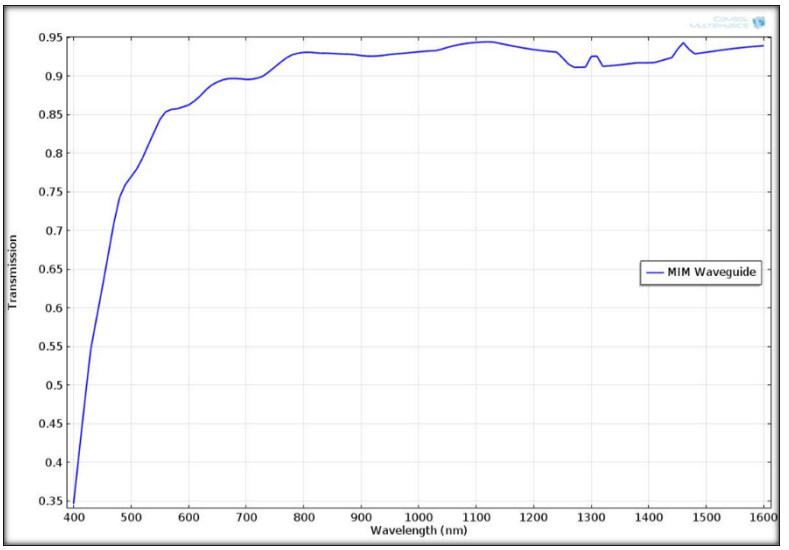

Fig 2. Waveguide transmission diagram (MIM) with a width of 100nm.

2.1 THE EFFECT OF CHANGING THE WAVEGUIDE WIDTH

To further investigate the propagation of waves inside MIM waveguides, we simulated the structure with four different widths of 25, 50, 100 and 150 nm for the waveguide. The simulation results show that as the width of the waveguide increases, its transmission spectrum becomes more efficient and less fluctuations are observed in it. Figure (3) shows the MIM waveguide transmission diagram for 4 different waveguide widths. In this case, the metal is silver and the inside the waveguide has a refractive index of 1. In the following simulations, we chose a width of 100 nm as the reference width for the waveguide.

2. 2 THE CHANGE OF METAL TYPE IN MIM WAVEGUIDE

The surface plasmon waves that are caused by the proximity of metal and insulator are dependent on factors such as the type of metal and the type of insulator. Here, instead of using silver to surround the waveguide, we used gold and aluminum to better comprehend the impacts of the metal material. Figure (4) shows the transmission diagram of MIM waveguide with a width of 100 nm for three different metals (silver, gold, and aluminum). From the figure, it is evident that the use of gold metal resulted in the structure having no transmission up to a wavelength of 500 nm, whereas the transmission effectiveness of aluminum metal was not less than 60%. From now on, in our simulation process, we have used silver metal as a reference metal in all structures.

2.3 THE CHANGE OF INSULATOR MATERIAL IN MIM WAVEGUIDE

As in the previous section, we examined the effect of the metal material on the optical response of the MIM waveguide, in this section, we also changed the insulator used inside the waveguide and compared the transmission diagram of the structure. In a behavior similar to the previous case, when we changed the insulator of the waveguide from air with a refractive index of 1 to materials such as SiO_2 and SiO, the transmission diagram showed a lower efficiency. In this case, the SiO material has the lowest transmission at the beginning of the wave range. It should be noted that in all the three cases tested, the metal used is silver and the width of the waveguide is 100 nm, and we used the same air insulator as the material inside the waveguide. Figure (5) shows the MIM waveguide transmission diagram for three different materials inside the waveguide.

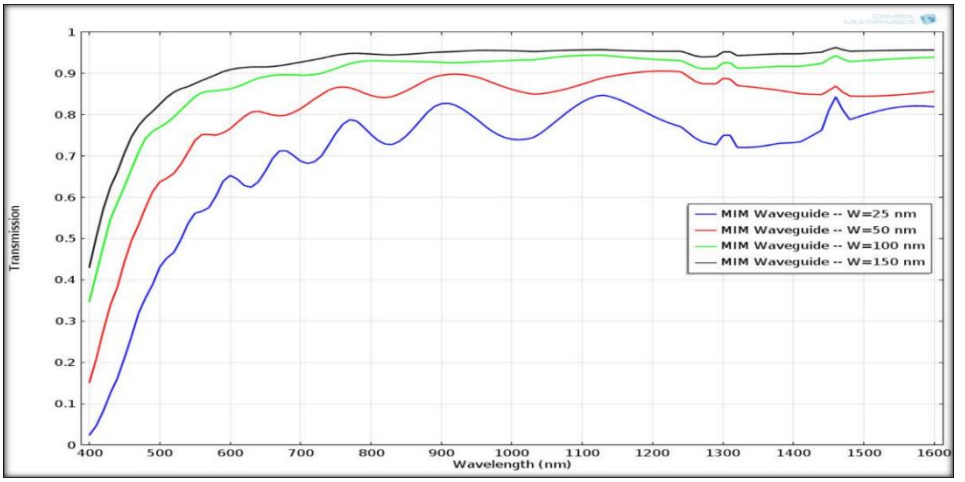

Fig 3. Transmission diagram of MIM waveguide for four different widths for waveguide.

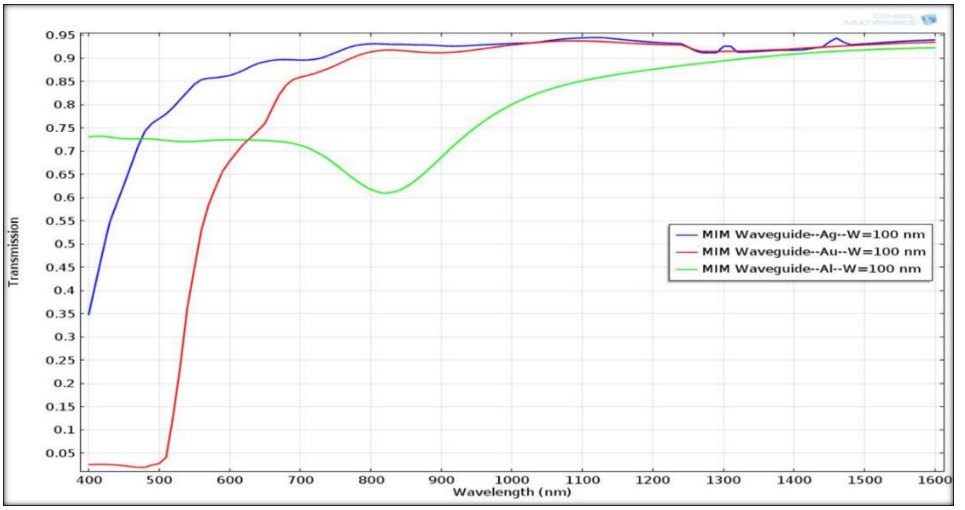

Fig 4. 100 nm wide waveguide transmission diagram (MIM) for three different metals.

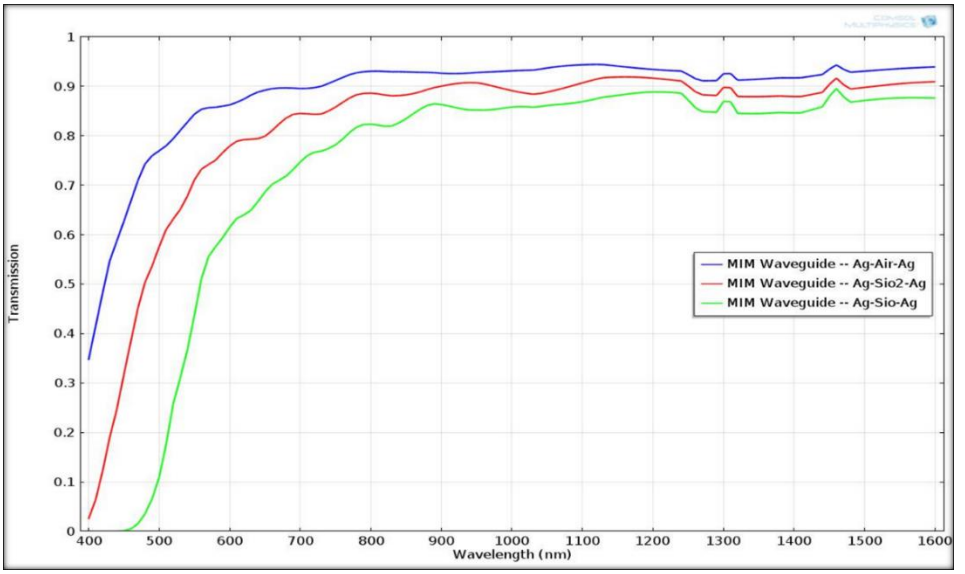

Fig 5. Transmission diagram of MIM waveguide with 100 nm width for different insulator material.

In the continuation of the investigation of MIM waveguides and plasmonic structures, an idea has been proposed that it is possible to create this plasmonic structure in the reverse form, i.e. insulator-metal-insulator (IMI) waveguide. To find the answer to this question, we conducted an experiment in which silver metal with a width of 100 nm was placed as the path of light propagation and we chose a surrounding material made of air. In this way, the waveguide structure was formed as IMI. Figure (6) compares the transmission diagram of MIM and IMI waveguides. It is obvious that our waveguide has no transmission when using the IMI structure and is not suitable for filtering and sensor applications. In this section, we investigated the property of surface Plasmon polarities (SPP) propagation in a cylindrical waveguide to which a resonator is vertically connected. Connecting this resonator to the main waveguide causes the excited SPP waves to propagate along the surface of the metal layer with a resonant mode inside the waveguide. In the case where a simple MIM waveguide was

used, it was observed that no resonance occurred in the waveguide transmission diagram and the waveguide transmitted light in the entire optical range. The resonator stub connected to the main waveguide has the same width as the waveguide itself, w=100nm and height H=300nm (Fig.7). Figure (8) shows the transmission diagram of the MIM waveguide with the resonator stub connected to it. As can be seen, the transmission diagram compared to the transmission diagram of the MIM waveguide without resonator has a drop at the wavelength of 570 nm. When the SPPs are passing through the waveguide, part of these waves are propagated into the coupled stub, then, the SPPs reflected from the end of the coupled stub interfere with the SPPs passing through the main waveguide and lead to this they fall In Fig.9 you can see the distribution of the field corresponding to the peaks and valleys of the transmission diagram of this waveguide.

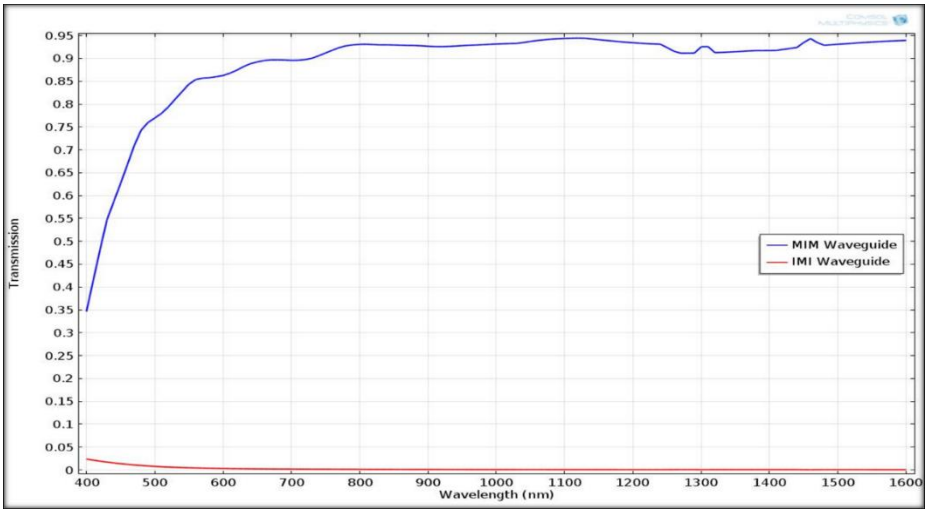

Fig 6. Transmission diagram of MIM waveguide and IMI waveguide, both with a width of 100 nm.

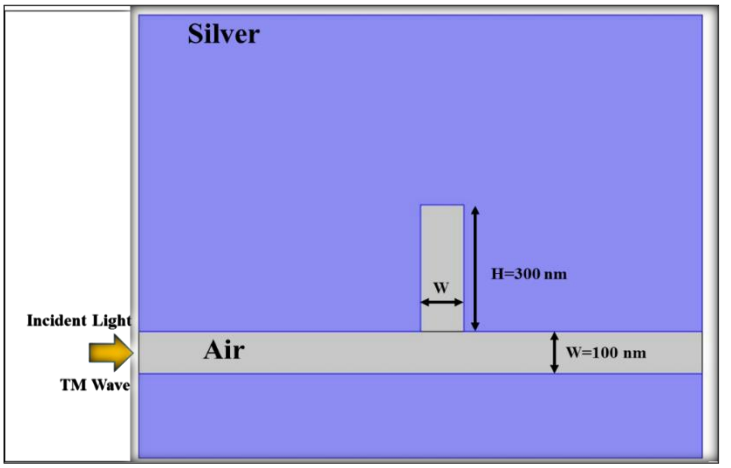

Fig 7. MIM waveguide structure with vertical resonator.

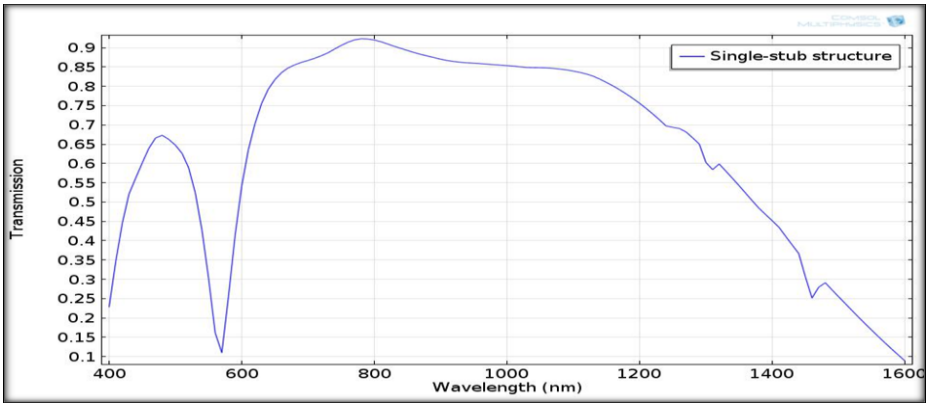

Fig 8. Transmission diagram of the MIM waveguide connected to the vertical resonator stub.

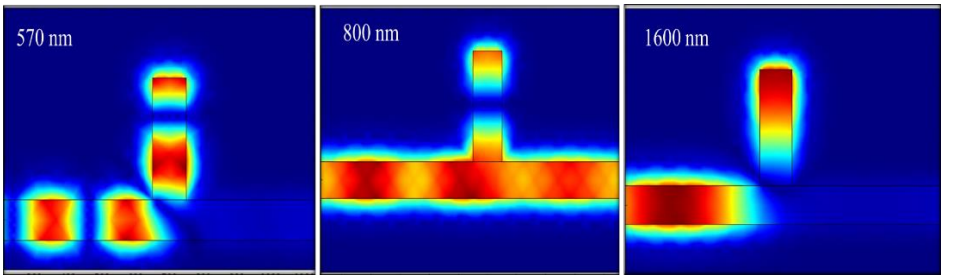

Fig 9. Field distribution corresponding to peaks and valleys of transmission diagram of MIM waveguide with vertical resonator.

2.4 THE DEFORMATION OF THE RESONATOR STUB IN THE MIM WAVEGUIDE

Plasmonic is based on the process of interaction between electromagnetic waves and conduction electrons in metals, Plasmonic can be used for applications in nonlinear optics which, due to the high field intensity in the plasmonic waveguides. [16, 17]

Since plasmonic structures and especially plasmonic waveguides have many applications in the design of optical components, so far a lot of research has been done in the field of optimizing and controlling the optical response of these waveguides. Each of the researches presented a method to control the transmission spectrum of waveguides. One of the methods presented in the field of controlling SPP waves and ultimately controlling the resonance wavelength is changing the shape of the resonators connected to them. Here we also compared the waveguide structure under simulation for rectangular and triangular resonator stack to investigate the propagation of SPP waves inside the waveguide and how the resonance modes change in the transmission diagram. In the rectangular resonator which was discussed in the previous section, the width of W=100nm and its height H=300nm was set, and in the triangular resonator connected to the waveguide, the width of the triangle was W=100nm and its height H=200nm. Figure (10) shows the MIM waveguide structure with two different stub shapes next to each other. The transition diagram of these two structures is shown in Fig.11. From this diagram, it is clear that the geometrical change of the stub connected to the waveguide significantly changes the waveguide transmission diagram. This change in the shape of the stub from rectangle to triangle has led to the resonance mode shift from 570nm to 950nm and also after the resonance mode, the transmission graph has not reached zero and has an efficiency of 60% or higher. From this change, we can conclude that the use of this stub geometry offers a promising method to single-mode the transfer diagram for use in filters.

2.5THE EFFECT OF CHANGING THE REFRACTIVE INDEX OF THE MATERIAL INSIDE THE WAVEGUIDE CONNECTED TO THE RESONATOR SHAFT

In the previous section, it was briefly explained that there are different methods to change and manipulate the optical response of plasmonic waveguides. Another of these methods is changing the refractive index of the material inside the waveguide. This change in refractive index also indicates that cylindrical MIM waveguides can be good refractive index sensors. In order to prove this issue, we subjected the MIM waveguide connected to the rectangular resonator

stub to the simulation under the conditions of changing the refractive index. In this experiment, the refractive index of the material inside the waveguide was changed to 1, 1.1, 1.2 and 1.3. Figure (12) shows the transmission diagram of the MIM waveguide connected to the rectangular resonator stub for different values of the refractive index of the material inside the waveguide. It is known that with the increase of the refractive index of the waveguide, the resonant mode has shifted to the right in the transmission spectrum. This result is very promising for the use of waveguides in refractive index sensors.

2.6THE EFFECT OF THE DISTANCE BETWEEN THE RESONATOR AND THE MAIN WAVEGUIDE

It has been shown in various researches that the coupling distance between the resonator stub and the main waveguide is an important and influential factor in the transmission properties of the waveguide. To show the effect of this distance on the propagation of SPP waves, we simulated the resonator stub connected to the main transducer for two distances of 10 and 20 nm from the waveguide and compared it with the case without the distance. The simulation results demonstrate that the resonant mode in the transmission spectrum, which was caused by the coupling between the SPPs reflected from the stub and the SPPs traveling through the waveguide, vanishes and changes as the distance between the stub and the main waveguide is increased. It is expected that with a large coupling distance between the stub and the waveguide, the transmission diagram returns to the initial state (the waveguide without the stub). Figure (13) shows the transmission diagram of the MIM waveguide connected to the resonator stub at different coupling distances between the stub and the waveguide. The blue line corresponds to the case where there is no gap.

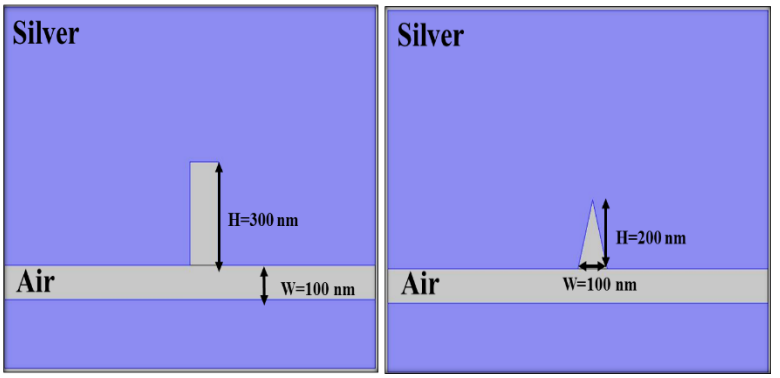

Fig 10. MIM waveguide structure with two rectangular and triangular resonator stubs.

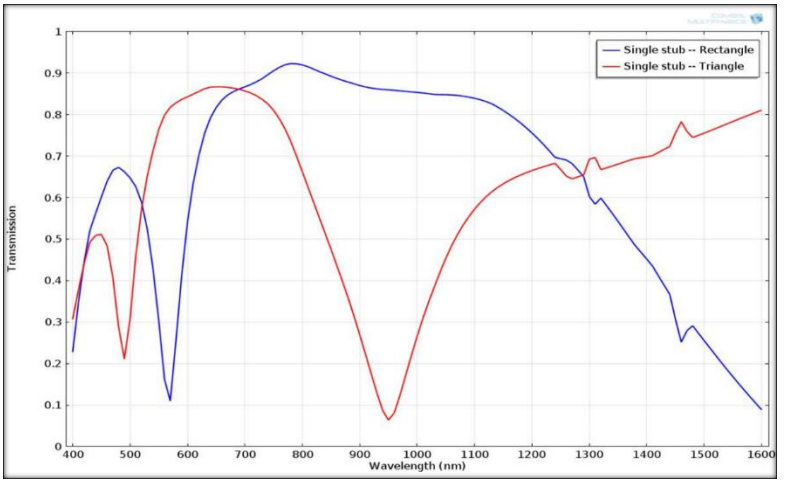

Fig 11. Transmission diagram of the MIM waveguide connected to the resonator stub with two geometries, rectangle and triangle.

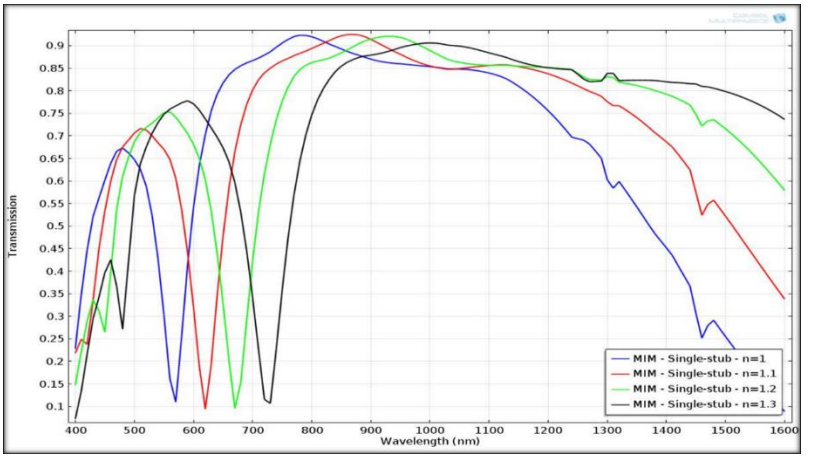

Fig 12. Transmission diagram of the MIM waveguide connected to the resonator stub for different refractive index values.

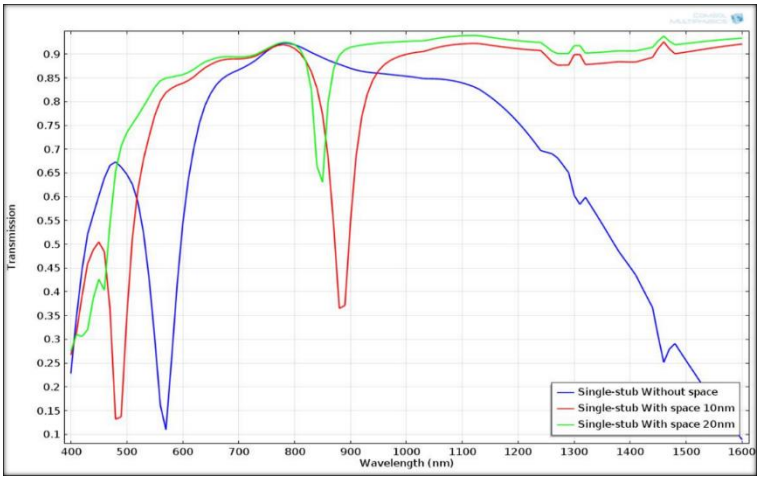

Fig 13. Transmission diagram of the MIM waveguide connected to the resonator stub for different connection distances.

2.7 Investigating the propagation of SPPs in the waveguide connected to the resonator stub and cavity

Another method of controlling the transmission spectrum of plasmonic waveguides and determining the number of resonant modes is to use a resonator cavity on top of the waveguide. This resonator cavity, which is placed on top of the stub, can also be effective in changing the transmission properties of the structure. To investigate the propagation of SPPs in the MIM waveguide connected to the vertical and horizontal resonators, we simulated these structures and by changing different parameters we evaluated and compared their effect on the transmission spectrum of the waveguide. For this purpose, we first placed a resonator cavity on top of the shaft connected to the waveguide and checked the transmission spectrum of the structure for the geometrical change of this added cavity (Fig. 14). Figure (15) shows the transfer diagram of rectangular and circular resonator. It can be seen that in both cases, the transmission spectrum has two resonant modes, one related to the stub and one related to the cavity above the stub.

2.8 The effect of changing the height of T-shaped resonator cavity in MIM waveguide

In this section, we will show how the transmission spectrum of the waveguide can be changed by changing the geometrical parameters of the resonator cavity, and by moving the resonance mode in the transmission diagram, we will be able to design the waveguide for our specific application. For this purpose, we

simulated the MIM waveguide which is connected to a T-shaped resonator cavity (Fig. 14) for different height H of the stub and simulated the resulting transmission diagrams. The simulation results showed that by increasing the height of the stub from 100 nm to 500 nm with a step of 100, the resonant modes in the transmission spectrum shifted to the right. Figure (16) shows the transition diagram of the structure for changing the height of the stub. Note that the cavity length L is fixed at 400 nm.

2.9 CHANGING THE LENGTH OF T-SHAPED RESONATOR CAVITY IN MIM WAVEGUIDE

In this step, we simulated the structure of the MIM waveguide connected to the cavity of the T-shaped resonator for different values for the length L of the cavity. At this stage, the height of the stub H is kept constant at 300 nm. As a result, similar to the result of height change, length change also led to the right shift of resonant modes in the transmission spectrum. Figure (17) shows the transmission diagram of the MIM waveguide connected to the T-shaped resonator cavity for changing the length of the horizontal cavity.

2.10THE NUMBER OF T-SHAPED HOLES IN THE MIM WAVEGUIDE

One of the other influential factors in the propagation of SPP waves inside waveguides is the change in the number of resonator cavities. Increasing the number of cavities leads to finding more resonant modes in the transmission spectrum, which is useful in filters and systems with high bandwidth to separate channels from each other. Figure (18) (a) to (d) respectively show the MIM waveguide structure with two resonator cavities, its transmission diagram, and the fields corresponding to the transmission diagram.

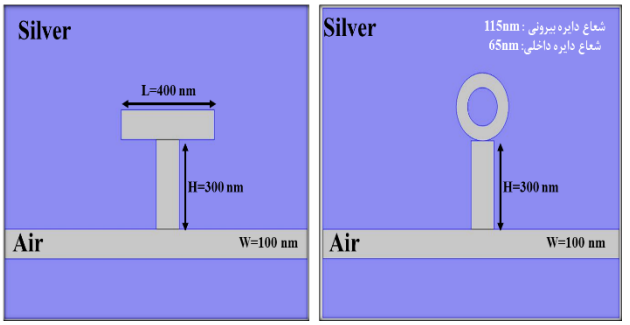

Fig 14. MIM waveguide structure connected to rectangular and circular resonator.

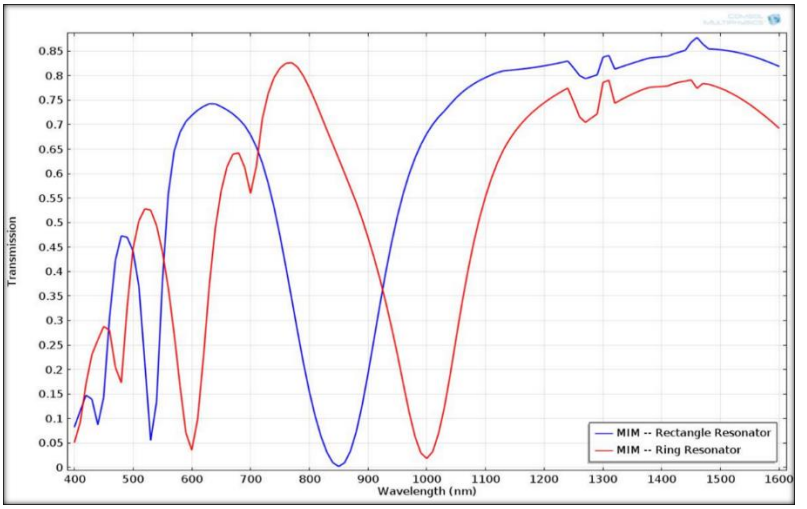

Fig 15. Transmission diagram of MIM waveguide connected to stub and resonator cavity with different geometric shape.

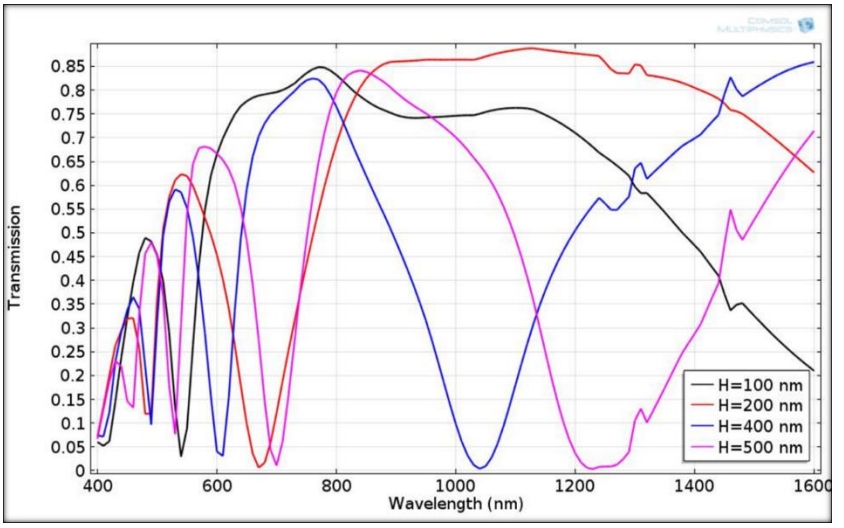

Fig 16. Transmission diagram of MIM waveguide connected to T-shaped resonator cavity with different height.

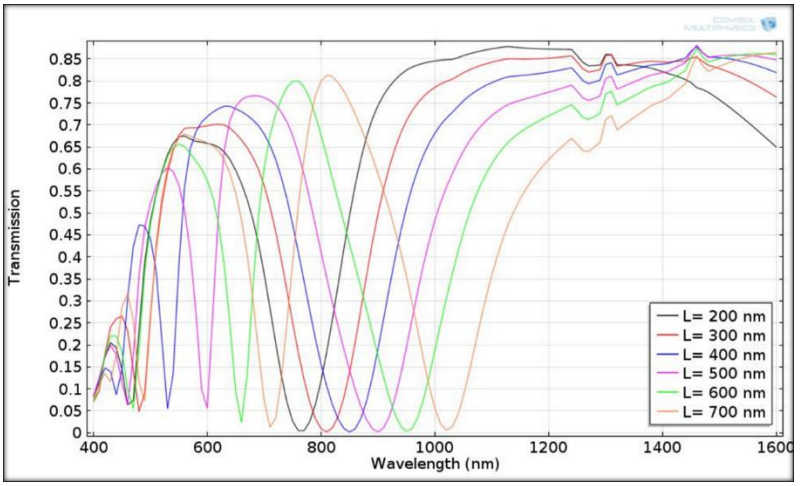

Fig 17. Transmission diagram of MIM waveguide connected to the T-shaped cavity for changes in the length of the horizontal cavity L.

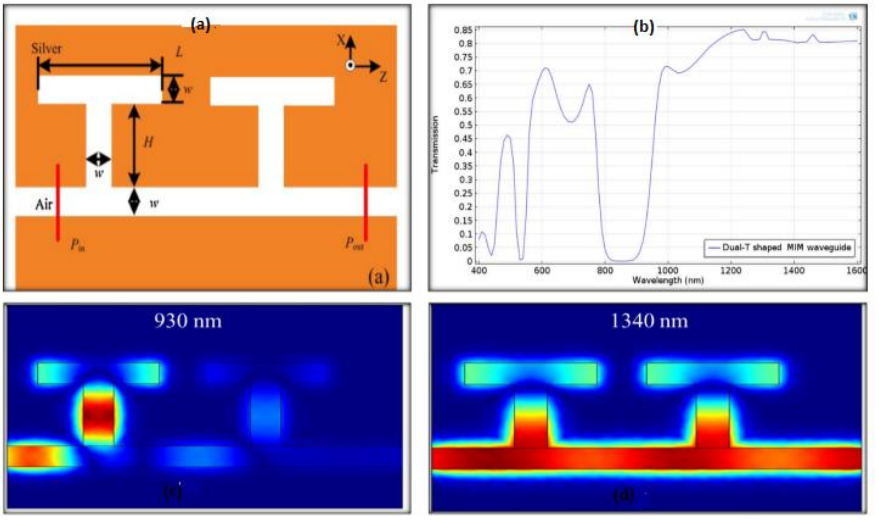

Fig 18. Structure, transmission diagram, field distribution corresponding to transmission diagram, for MIM waveguide connected to two T-shaped resonator cavities.

3. CONCLUSION

In this paper, the characteristics of surface plasmon polarization propagation in a cylindrical waveguide were investigated. When the waveguide did not use any resonator, its transmission spectrum never reached zero, even after the wavelength of 800nm, its transmission efficiency was over 90%. The reason for this complete transmission spectrum is that the emitted light and the resonant wavelength of the structure are far apart and there was no interference between them. Further, as we increased the width of the waveguide, its transmission spectrum became more efficient and less fluctuations were observed in it. Then we showed the transmission spectrum of MIM waveguide with a width of 100 nm for three different metals, silver, gold, and aluminum. It was clearly observed that the use of gold metal caused the structure to have no transmission up to the wavelength of 500 nm, while the transmission efficiency in aluminum metal was not lower than 60% in the entire optical range. Therefore, silver metal was used as the best reference metal in all structures. Then we changed the insulator of the waveguide from air with a refractive index of 1 to materials such as SiO_2 and SiO, the transmission diagram showed a lower efficiency. So air was the best option. To further investigate the plasmonic structure in reverse form i.e. insulator-metal-insulator waveguide We also created IMI, which we saw that if we use the IMI structure, our waveguide has no transmission and is not suitable for filtering and sensor applications. [20,21]

In the subsequent study, the properties of surface plasmon polaritons emission were investigated in the case where a resonator is vertically connected to[18] it. The transmission diagram had a drop in the wavelength of 570 nm compared to the MIM waveguide without resonator. When the SPPs are passing through the waveguide, part of these waves are propagated into the coupled stub, then the SPPs reflected from the end of the coupled stub interfere with the SPPs passing through the main waveguide and lead to This drop is transmitted in the graph. Then we compared the waveguide structure under simulation for the rectangular and triangular resonator shaft. It was observed that the geometrical change of the shaft connected to the waveguide significantly changes the waveguide transmission diagram. This change of the shape of the stub from rectangle to triangle has led to the shift of resonance mode from 570nm to 950nm. Also, after the intensification mode, the transfer graph does not reach zero and has an efficiency of 60% or higher. From this change, it can be concluded that to single-mode the transmission diagram for use in filters, the use of this stub geometry provides a promising method. For further investigation, the effect of changing the refractive index of the material inside the waveguide connected to

the resonator stub was investigated and it was found that with the increase of the refractive index of the waveguide, the resonance mode shifted to the right in the transmission spectrum. This result is very promising for the use of waveguides in refractive index sensors. By examining the effect of the distance between the resonator stub and the main waveguide, it was observed that with the increase of the distance between the stub and the main waveguide, the resonance mode in the transmission spectrum, which was the result of the coupling between the SPPs reflected from the stub and the SPPs passing through the waveguide, disappeared and shifted. By examining the effect of changing the length of the cavity of the T-shaped resonator, it was observed that the change in length also led to the shift of resonance modes to the right in the transmission spectrum, and finally, by examining the effect of the number of T-shaped cavities, it was observed that this increase in the number of cavities led to finding more resonant modes in the transmission spectrum. It is possible that this issue has a good use in filters and systems with high bandwidth to separate channels from one another.[22]

REFERENCES

[1] M. G. Saber, R. H. Sagar, M. T. Al-Amin & A. Al Noor. *Investigation of propagation properties of Surface Plasmon Polariton mode in AlGaAs/Ag/AlGaAs waveguide*. Presented at 2nd International Conference on Advances in Electrical Engineering (ICAEE), (2013) 33-36.

Available: https://ieeexplore.ieee.org/abstract/document/6750300

[2] G. Xiao, X. Wang & Z. Zhou. *Propagation Properties of Symmetric Surface Plasmon Polaritons Mode in Waveguide*. IEEE Photonics Technology Letters. 24 (8) (2012) 628-630.

Available: https://ieeexplore.ieee.org/abstract/document/6130591

[3] H. Yang, J. Li & G. Xiao. *Decay and propagation properties of symmetric surface plasmon polariton mode in metal–insulator–metal waveguide*. Optics Communications. 395 (2017) 159-162.

Available: https://www.sciencedirect.com/science/article/abs/pii/S0030401815302443

[4] Z. Han & S. I. Bozhevolnyi. *Waveguiding with surface plasmon polaritons*. In Handbook of Surface Science. North-Holland, 2014, 137-187. Available: https://www.sciencedirect.com/science/article/abs/pii/B9780444595263000057

[5] V. K. Sharma, A. Kumar & A. Kapoor. *Analysis of surface and guided wave plasmon polariton modes in insulator–metal–insulator planar plasmonic waveguides*. Optics Communications. 285 (6) (2012) 1123-1127.

Available:
https://www.sciencedirect.com/science/article/abs/pii/S0030401811011928

[6] A. Sellai & M. Elzain. *Features of a insulator-metal-insulator plasmonic waveguide with a double grating*. Presented at IEEE International Conference on Signal Processing and Communications (2007) 852-855. Available:

https://www.researchgate.net/publication/261270931_Features_of_a_Dielectric-Metal-Dielectric_Plasmonic_Waveguide_with_a_Double_Grating

[7] Z. Zhang, Z. Zhang & H. Wang. *The effect of the metal cylinder in the slot on the transmission properties of the metal–insulator–metal waveguide*. Journal of Optoelectronical Nanostructures. 124 (23) (2013) 6351-6354.

Available:
https://www.sciencedirect.com/science/article/abs/pii/S003040261300716X

[8] H. Yu, C. Sun, H. Tang, X. Deng & J. Li. *A surface-plasmon-polariton wavelength splitter based on a metal–insulator–metal waveguide*. Photonics and Nanostructures-Fundamentals and Applications. 12 (5) (2014) 460-465.

Available:
https://www.sciencedirect.com/science/article/abs/pii/S1569441014000492

[9] L. Salomon, F. Grillot, A. V. Zayats & F. De Fornel. *Near-field distribution of optical transmission of periodic subwavelength holes in a metal film*. Physical review letters. 86 (6) (2001) 1110.

Available:
https://journals.aps.org/prl/abstract/10.1103/PhysRevLett.86.1110

[10] M. Olyaee, M. B. Tavakoli & A. Mokhtari. *Propose, Analysis and Simulation of an All Optical Full Adder Based on Plasmonic Waves using Metal-Insulator-Metal Waveguide Structure*. Journal of Optoelectronical Nanostructures Review B. 54 (9) (2019) 6227.

Available:
https://journals.marvdasht.iau.ir/article_3622_345ca515d72d1b069f68df919aba7b29.pdf

[11] S. I. Bozhevolnyi, J. Erland, K. Leosson, P. M. Skovgaard & J. M. Hvam. *Waveguiding in surface plasmon polariton band gap structures*. Physical review letters. 86 (14) (2001) 3008.

Available: https://journals.aps.org/prl/abstract/10.1103/PhysRevLett.86.3008

[12] L. Hajshahvaladi, H. Kaatuzian, M. Danaie & A. A. Nohiji. *The effect of metal rods in a hybrid plasmonic-photonic crystal cavity design*. Presented at 30th International Conference on Electrical Engineering (ICEE), (2022) 936-940.

Available: https://ieeexplore.ieee.org/abstract/document/9827340

[13] M. Mansouri, A. Mir & A. Ali Farmani. *Numerical Modeling of a Nanostructure Gas Sensor Based on Plasmonic Effec*. Journal of Optoelectronical Nanostructures. 4 (2) (2019, Spring).

Available: https://journals.marvdasht.iau.ir/article_3476_087a7e56aefeafb4744d557b38f01339.pdf

[14] S. G. Shafagh, H. Kaatuzian & M. Danaie. *Analysis, design and simulation of MIM plasmonic filters with different geometries for technical parameters improvement*. Communications in Theoretical Physics. 72 (8) (2020) 085502.

Available: https://iopscience.iop.org/article/10.1088/1572-9494/ab95f8/meta

[15] U. Kreibig & M. Vollmer. *Theoretical Considerations. In:* Kreibig, U. & Vollmer, M. (eds.) Optical Properties of Metal Clusters. Berlin, Heidelberg: Springer Berlin Heidelberg, 1995, 13-201. Available: https://books.google.com/book

[16] M. Dehghani, M. Hatami & A. Gharaati. *Supercontinuum Generation in Silica Plasmonic Waveguide by Bright Soliton*. Journal of Optoelectronical Nanostructures. 6 (4) (2021) 109-136.

Available: https://jopn.marvdasht.iau.ir/article_5053_091fd039a5a3443e083aadc2211eab32.pdf

[17] K. Zarei, G. Solookinejad & M. Jabbari. *Investigating the Properties of an Optical Waveguide Based on Photonic Crystal with Point Defect and Lattice Constant Perturbation*. The Quarterly Journal of Optoelectronical

Nanostructures. 1 (1) (2016, Spring) 65-80. Available: https://jopn.marvdasht.iau.ir/article_1816.html

[18] G. G. Zheng, L. H. Xu, Y. Z. Liu & W. Su. *Optical filter and sensor based on plasmonic-gap-waveguide coupled with T-shaped resonators*. Journal of Optoelectronical Nanostructures. 126 (23) (2015) 4056-4060.

Available: https://www.sciencedirect.com/science/article/abs/pii/S0030402615007597

[19] B. Laks, D. L. Mills & A. A. Maradudin. *Surface polaritons on large-amplitude gratings*. Physical Review B. 10 (1981) 4965.

Available: https://journals.aps.org/prb/abstract/10.1103/PhysRevB.23.4965

[20] V. a. G. Rivera, O. B. Silva, Y. Ledemi, Y. Messaddeq & E. Marega. *Plasmonic Nanostructure Arrays Coupled with a Quantum Emitter*. *In:* Rivera, V. a. G., Silva, O. B., Ledemi, Y., Messaddeq, Y. & Marega Jr, E. (eds.) Collective Plasmon-Modes in Gain Media: Quantum Emitters and Plasmonic Nanostructures. Cham: Springer International Publishing, 2015, 71-116.

Available: https://link.springer.com/book/10.1007/978-3-319-09525-7

[21] J. Jacob, A. Babu, G. Mathew & V. Mathew. *Propagation of surface plasmon polaritons in anisotropic MIM and IMI structures*. Superlattices and microstructures. 44 (3) (2008) 282-290.

Available: https://www.sciencedirect.com/science/article/abs/pii/S0749603608001092

[22] A. Abdikian, G. Solookinejad & Z. Safi. *Electrostatics Modes in Mono-Layered Graphene*. Journal of Optoelectronical Nanostructures Summer. 1 (2) (2016). Available: https://jopn.marvdasht.iau.ir/article_2044_8b18c60167baa91a0369f64730d82f40.pdf